

# Measurement of negative particle multiplicity in S-Pb collisions at 200 GeV/c per nucleon with the NA36 TPC

## NA36 Collaboration

E. Andersen<sup>1,a</sup>, R. Blaes<sup>2</sup>, J.M. Brom<sup>2</sup>, M. Cherney<sup>3</sup>, B. de la Cruz<sup>4</sup>, C. Fernández<sup>5,\*</sup>, C. Garabatos<sup>5,b</sup>, J.A. Garzón<sup>5</sup>, W.M. Geist<sup>2</sup>, D.E. Greiner<sup>6</sup>, C.R. Gruhn<sup>6,c</sup>, M. Hafidouni<sup>2,d</sup>, J. Hrubec<sup>7</sup>, P.G. Jones<sup>6</sup>, E.G. Judd<sup>8,e</sup>, J.P.M. Kuipers<sup>9,f</sup>, M. Ladrem<sup>2,g</sup>, P. Ladrón de Guevara<sup>4</sup>, G. Løvhøiden<sup>1</sup>, J. MacNaughton<sup>7</sup>, J. Mosquera<sup>5</sup>, Z. Natkaniec<sup>10</sup>, J.M. Nelson<sup>8</sup>, G. Neuhofer<sup>7</sup>, C. Pérez de los Heros<sup>4,h</sup>, M. Pló<sup>5</sup>, P. Porth<sup>7</sup>, B. Powell<sup>9</sup>, A. Ramil<sup>5</sup>, H. Rohringer<sup>7</sup>, I. Sakrejda<sup>6</sup>, T.F. Thorsteinsen<sup>1,\*</sup>, J. Traxler<sup>7</sup>, C. Voltolini<sup>2</sup>, K. Wozniak<sup>10</sup>, A. Yañez<sup>5</sup> and R. Zyberty<sup>8,i</sup>.

- 1) University of Bergen, Dept. of Physics, N-5007 Bergen, Norway.
- 2) Institut de Recherches Subatomiques (IReS), IN2P3-CNRS/Université Louis Pasteur, B.P. 28, F-67037 Strasbourg Cedex 2, France.
- 3) Creighton University, Dept. of Physics, Omaha, Nebraska 68178, USA.
- 4) CIEMAT, Div. de Física de Partículas, E-28040 Madrid, Spain.
- 5) Universidad de Santiago, Dpto Física de Partículas, E-15706 Santiago de Compostela, Spain.
- 6) Lawrence Berkeley Laboratory (LBL), Berkeley CA 94720, USA.
- 7) Institut für Hochenergiephysik (HEPHY), A-1050 Wien, Austria.
- 8) University of Birmingham, School of Physics and Space Research, Birmingham B15 2TT, UK.
- 9) European Organization for Nuclear Research (CERN), CH-1211 Genève 23, Switzerland.
- 10) Instytut Fizyki Jadrowej, PL-30 005 Kraków 30, Poland.
- a) Present address: Haukeland Sykehus, Med.-tek. avd., N-5021 Bergen, Norway.
- b) Present address: GSI, Darmstadt, Germany.
- c) Present address: CERN, PPE division.
- d) Present address: 50, Rue de Soultz, 67100 Strasbourg, France.
- e) Present address: LBL, USA.
- f) Present address: ETH, Zürich, Switzerland.
- g) Present address: Ecole Normale Supérieure, Algiers, Algeria.
- h) Present address: University of Uppsala, Uppsala, Sweden.
- i) Present address: ZYBERT Computing Ltd, Birmingham B32 3PW, UK.

---

\* Deceased.

**Abstract.** A high statistics study of the negative particle multiplicity distribution from S-Pb collisions at 200 GeV/c per nucleon is presented. The NA36 TPC was used to detect charged particles; corrections are based upon the maximum entropy method.

## Introduction.

Experiments with ultrarelativistic nucleus-nucleus collisions may lead to the discovery of a new state of matter: the quark gluon plasma. Various experiments involved in this program are both investigating different predicted plasma signatures and trying to understand the dynamics of these collisions in general. With this in mind various features are studied; among them multiplicity distributions.

Here a measurement of the inclusive multiplicity distribution of negative particles produced in S-Pb collisions at 200 GeV/c per nucleon [1] is presented; it was obtained by the NA36 Time Projection Chamber (TPC) designed for the high multiplicity environment of heavy-ion collisions. Detection inefficiencies were corrected for using a maximum entropy method.

## The experimental apparatus.

The NA36 spectrometer consisted of a TPC [2] and a set of detectors originating from the former European Hybrid Spectrometer [3]. Only the detectors relevant to the multiplicity measurement are described here. The Pb target (5% of an interaction length) is surrounded by two triggering Si counters located 20 cm upstream and downstream. The one upstream selects the incident beam S ions, whereas the one downstream rejects those S ions having not interacted in the target. This rejection, based on the amplitude of the signal, defines the "minimum bias" event sample. The target and the Si detectors are placed inside a vacuum tank extending up to the TPC in order to minimize secondary interactions.

The TPC has a volume of  $50 \times 50 \times 100 \text{ cm}^3$ ; its electric field is parallel to a strong horizontal magnetic field (2.7 T) produced by a superconducting magnet. The TPC is installed 1 cm above the beam line and 1 m downstream of the target in order to avoid most nuclear fragments in its sensitive volume. Because of the strong magnetic field and the position of the TPC, most of the detected particles have the same charge sign. The TPC is read out by a matrix of 1 cm long anode wires, organized in 40 vertical rows of 192 wires each. The wire and row pitches are 0.1 inch and 1 inch, respectively. Two-track resolutions of  $\sigma_Y^t = 5 \text{ mm}$  and  $\sigma_Z^t = 10 \text{ mm}$ , in the vertical direction of the bend plane and the drift direction, respectively, were obtained [2]. Data were taken with two magnetic field polarities.

The acceptances of the TPC in terms of laboratory rapidity  $y$  and transverse momentum  $P_T$  are shown in the figure 1. They were derived from Monte-Carlo simulations to be discussed below. In the

following only the vertex tracks with  $2 \leq y \leq 5$ ,  $0.1 \leq P_T \leq 2 \text{ GeV}/c$  and  $-89^\circ \leq \varphi \leq 89^\circ$  ( $\varphi$  is the azimuthal angle) will be considered. These restrictions were made in order to avoid large corrections.

### **Selection of events.**

The results presented here are based on about 14000 minimum bias events. The hits recorded by the TPC were used to reconstruct and fit tracks by the usual track road and track following methods [4]. The position of the primary vertex was determined by the Kalman filter method [5]. Its distribution along the beam axis (Fig. 2) agrees with Monte-Carlo simulations. Contamination from interactions outside the target has been removed from our data sample by rejecting vertices with  $X < -115 \text{ cm}$  and  $X > -109 \text{ cm}$ .

Contamination from electromagnetic dissociation (EMD) was removed from the sample of events without any vertex tracks observed in the TPC. Its contribution was calculated from the charge changing and the production cross-sections measured by NA36 [6] and estimated elsewhere [7]; about  $36.5 \pm 6.1\%$  of the minimum bias events are due to EMD. All results reported in the following refer therefore, to the strong inelastic cross section.

### **Correction of the multiplicity distribution.**

The observed negative multiplicity distribution has to be corrected for efficiency and geometrical acceptance of the TPC, as well as for inelastic reinteractions in the target and downstream of it. For an observed multiplicity distribution  $O$  of  $M$  bins and the true one,  $T$ , of  $N$  bins one arrives at the following relation [8,9]:

$$O_m = \sum_{n=1}^N P_{mn} T_n, \quad (1)$$

where  $O_m$  ( $m = 1, \dots, M$ ) is the fraction of events with observed negative multiplicity in the bin  $m$  and  $T_n$  is the fraction of events with true negative multiplicity in the bin  $n$ ;  $P_{mn}$  is the probability that an event with a true multiplicity in the bin  $n$  be observed as an event with observed multiplicity in the bin  $m$ . Hence, the  $P_{mn}$  satisfy the following relation:

$$\sum_{m=1}^M P_{mn} = 1. \quad (2)$$

The matrix  $P$  was determined from a Monte-Carlo simulation of S-Pb interactions, based on 23000 IRIS events [10], and which included a GEANT simulation of reinteractions in all parts of the experimental setup (target, TPC, ...), as well as a simulation of signal formation in the TPC and of reconstruction and analysis programs. The momenta of simulated tracks at the primary vertex were used to establish the acceptances discussed above.

The underconstrained system of equations (1) cannot be solved in a straightforward way; this may lead to some negative values of  $T_n$ . Since the bins' contents are subject to statistical fluctuations, one should, rather, look for a solution  $(T_1, \dots, T_N)$  that describes the data well in a statistical sense, which means that the differences  $\left|O_m - \sum_{n=1}^N P_{mn} T_n\right|$  are of the order of the corresponding statistical errors  $\sigma_m$  and not equal to zero as would be the case if (1) is solved directly.

The usual procedure (least squares fit) consists in minimizing

$$\chi^2 = \sum_{m=1}^M \left( \frac{O_m - \sum_{n=1}^N P_{mn} T_n}{\sigma_m} \right)^2. \quad (3)$$

This method yields unstable solutions [8,9,14].

An alternative method to choose one probability distribution from a set of distributions compatible with the data requires maximizing the Shannon entropy [11]

$$S = - \sum_{n=1}^N t_n \ln t_n, \quad t_n = \frac{T_n}{\sum_{i=1}^N T_i} \quad (4)$$

under constraints imposed by the data. This is known as the principle of maximum entropy, proposed by E.T. Jaynes [12]. It has been shown that the maximum entropy method (MEM) is the only consistent method of inference for underconstrained problems [13]. The MEM has been used earlier for the correction of measured multiplicity distributions [8,9,14,15].

Here, the observed multiplicity was corrected as in ref. [14]. The constraints were chosen by requiring that the moments of the observed distribution be reproduced by the true one, i.e.

$$\sum_{m=1}^M m^q O_m = \sum_{m=1}^M \sum_{n=1}^N m^q P_{mn} T_n \quad (5)$$

for some values of  $q$ . The choice of moments was motivated by the fact that they are less sensitive to statistical fluctuations than individual bins. The number of constraints (i.e. number of different moments) was selected such that

$$\chi^2 \approx M, \quad (6)$$

where the  $\chi^2$  is given by (3). A set of seven constraints corresponding to  $q = -1, 0, 1, \dots, 5$  was necessary.

## Discussion of the results.

Figure 3 shows the multiplicity distribution as it is obtained after the removal of the EMD contamination. This distribution will be corrected in the following in the TPC phase space:  $2 \leq y \leq 5$ ,  $0.1 \leq P_T \leq 2 \text{ GeV}/c$ ,  $-89^\circ \leq \varphi \leq 89^\circ$ , and in the full phase space. For each case the appropriate matrix  $P_{mn}$  was determined.

Figure 4 shows the corrected multiplicity distribution in the TPC phase space. The error bars are statistical. The mean negative multiplicity and the dispersion  $D_- = \sqrt{\langle n_-^2 \rangle - \langle n_- \rangle^2}$  are found to be

$$\langle n_- \rangle = 33.84 \pm 0.23 \quad (7)$$

$$D_- = 26.36 \pm 0.68 \quad (8)$$

and their ratio is

$$\frac{\langle n_- \rangle}{D_-} = 1.284 \pm 0.034 \quad (9)$$

Figure 5 shows the multiplicity distribution for full phase space; again the error bars are statistical. The mean multiplicity, dispersion and the ratio are now

$$\langle n_- \rangle = 57.01 \pm 0.39 \quad (10)$$

$$D_- = 44.04 \pm 0.82 \quad (11)$$

$$\frac{\langle n_- \rangle}{D_-} = 1.295 \pm 0.020 \quad (12)$$

As this distribution is inferred from the one measured in the TPC, it may depend on the model used for simulation [10]. A Monte-Carlo study of the rapidity distribution suggests that the systematic error of  $\langle n_- \rangle$  due to extrapolation to full phase space is of the order of 3.5%.

The corrected distributions have a maximum at low multiplicities corresponding to peripheral collisions, followed by a somewhat flat region ('plateau') for intermediate values of the impact parameter. At higher multiplicities a steep fall off ('tail'), due to central collisions is observed.

The corrected distributions are of about the same shape as those measured by other experiments, especially NA35 [16,17] and NA34 [18]. In particular, our distribution for S-Pb collisions is compatible with NA35 O-Au [16] distribution when given in terms of KNO variables. One observes, however, a discrepancy between the distributions in fig. 4 and fig. 5 and those reported by WA80 [19]. This can be explained by the fact that peripheral collisions were strongly suppressed in the data of ref. [19], whereas they are included in the present analysis.

A proportionality between  $D_-$  and  $\langle n_- \rangle$  (figure 6) from collisions of oxygen with different targets at energies of 60 and 200  $GeV/n$  were reported in ref. [16]. Added in figure 6 are the results from S-S and S-Cu collisions [17] as well as the present S-Pb measurement. All points tend to lie on a straight line. A similar proportionality had been observed long ago for pp collisions [20]. This proportionality was, in the case of nucleus-nucleus collisions, explained in terms of a superposition of independent nucleon-nucleus collisions [16].

Entropy is an alternative, useful variable for the study of multiparticle production [21,22]; it reflects general features of independent particle production. The total entropy from statistically independent

phase space regions, e.g. intervals  $\Delta y$ , is given by the sum of the entropies of these regions. Therefore, the total entropy  $S$  is proportional to the total rapidity range  $Y_m$ :  $S \sim Y_m$ . This is related to Feynman's argument on scaling in the variable  $\xi = y/Y_m$  [21]. In addition, it follows from eq. (4) that  $S$  is invariant under distortions of the multiplicity scale. An analysis of hadron-hadron collisions for  $\sqrt{s} > 20 \text{ GeV}$  shows that the entropy (4) increases linearly with the maximum rapidity  $Y_m$  of the produced pions [21]

$$\frac{S}{Y_m} = 0.417 \pm 0.009 \quad (13)$$

For S-Pb collisions in this experiment one finds

$$\frac{S}{Y_m} = 0.487 \pm 0.003 \quad (14)$$

where  $Y_m = \ln\left(\frac{\sqrt{s} - n_p m_n}{m_\pi}\right)$ ,  $m_\pi$  ( $m_n$ ) is the pion (nucleon) mass and  $\sqrt{s}^*$  is the center of mass energy of  $n_p$  ( $= A + \overline{B}$ ) participating nucleons. The maximum rapidity is obtained for central collisions, therefore  $Y_m^{S-Pb} = 8.76$  was used. (Note that  $Y_m^{p-p} = 4.93$  at  $200 \text{ GeV}/c$ ).

Šimák et al. [23] show also that multiparticle production exhibits a multifractal behaviour by investigating higher generalized fractal dimensions of order  $q$  given by

$$D_q = \frac{I_q}{Y_m} \quad (15)$$

where

$$I_q = \frac{1}{1-q} \ln\left(\sum_n t_n^q\right) \quad (16)$$

is the Rényi generalized entropy [24]. It can be shown that

$$\lim_{q \rightarrow 1} I_q = S \quad (17)$$

where  $S$  is given by (4). Figure 7 shows measured values of  $D_q$  for different values of  $q$ .  $D_q$  decreases with  $q$ , which may be considered as a signal of a multifractal behaviour in multiplicity distributions. This behaviour has also been found in ref. [25] for ion-emulsion interactions at various energies. The absolute values of  $D_q$  measured are smaller than those of ref. [25], which may be due to the values of  $Y_m$  for the AgBr target.

---


$$* \quad s = (\underline{P}_A + \underline{P}_B)^2,$$

where  $\underline{P}_A = (\sqrt{A^2 P_L^2 + (A m_n + \epsilon_A)^2}, \vec{P}_T = \vec{0}, A \vec{P}_L)$  and  $\underline{P}_B = (\overline{B} m_n + \epsilon_B, \vec{P} = \vec{0})$ ;

$\overline{B} = B - A[(B/A)^{2/3} - 1]^{3/2}$  is the number of participants in the target for central collisions.  $A$  and  $B$  are, respectively, the numbers of nucleons of projectile (sulphur) and target (lead),  $P_L = 200 \text{ GeV}/c$  and  $m_n$  is the rest mass of a nucleon; the binding energies  $\epsilon_A$  and  $\epsilon_B$  were neglected.

Generalized fractal dimensions  $D_q$  were also determined from the newly introduced Tsallis generalized entropy [26]:

$$I_q = k \frac{1 - \sum_n t_n^q}{q - 1} \quad (18)$$

with  $k = 1$  [26]; they are given in fig. 7 as well. (Note that  $I_q$  in (18) fulfills eq. (17)).

## **Conclusion.**

A high statistics study of fully inclusive negative multiplicity distributions from S-Pb collisions at 200  $GeV/c$  is presented both for limited and full phase space. A proportionality between  $\langle n_- \rangle$  and  $D_-$  is observed. The generalized fractal dimensions are shown to decrease with increasing order which may be interpreted as a multifractal behaviour of the multiplicity distribution.

## **Acknowledgements.**

One of us (M.H.) gratefully acknowledges helpful discussions with C. Fuglesang and M. Schmelling, and kind hospitality at IReS. Part of this work was supported by Director, Office of Energy Research, Division of Nuclear Physics Of the Office of High Energy and Nuclear Physics of the U. S. Department of Energy under contract no DE-AC03-76SF00098 (LBL), DE-FG02-91ER40652 (Creighton), DE-FG02-87ER40315 (CMU), by the United Kingdom Science and Engineering Council under grant GR/F 40065 and by the EC under contract A88000145. Authors are grateful to the CERN Directorate, the former CERN EP, EF, DD and SPS divisions and the CERN's PPCS group, and especially to D. Lord.

## **Note added in proof.**

The multiplicity distribution presented here is well fitted by the percolating string fusion model and by the generalized negative binomial model (S. Hegyi, private communication).

## References.

- [1] M. Hafidouni, Doctorat de l'Université Louis Pasteur de Strasbourg, CRN/HE 92-35 (1992).
- [2] C. Garabatos, Nucl. Instr. Meth. A283 (1989) 553.
- [3] M. Aguilar-Benitez et al., Nucl. Instr. Meth. 258 (1987) 26.
- [4] R.K. Bock, H. Grote, D. Notz and M. Regler, in: M. Regler (Ed.), Data Analysis Techniques in High Energy Physics, Cambridge University Press, Cambridge, 1990.
- [5] NA36 Collab., E. Andersen et al., Nucl. Instr. Meth. A301 (1991) 69.
- [6] NA36 Collab., E. Andersen et al., Phys. Lett. B220 (1989) 328.
- [7] C. Brechtmann and W. Heinrich, Z. Phys. A331 (1988) 463.
- [8] UA5 Collab., R.E. Ansorge et al., Z. Phys. C43 (1989) 357.
- [9] ALEPH Collab., D. Decamp et al., Phys. Lett. B273 (1991) 181.
- [10] J.-P. Pansart, Nucl. Phys. A261 (1987) 521c; Saclay Preprint DPhPE 89-04 (March 1989); in: J. Tran Thanh Van (Ed.), Proceedings of the 23rd Rencontre de Moriond, Editions Frontières, Gif-sur-Yvette, 1988.
- [11] C.E. Shannon, Bell Syst. Tech. J. 27 (1948) 379. This paper is reproduced in: D. Slepian (Ed.), Key Papers in The Development of Information Theory, IEEE Press, New-York, 1974.  
C.E. Shannon and W. Weaver, The Mathematical Theory of Communication, University of Illinois Press, Urbana, 1949.
- [12] E.T. Jaynes, Phys. Rev. 106 (1957) 620; 108 (1957) 171.
- [13] J.E. Shore and R.W. Johnson, IEEE Trans. Inf. Th. IT-26 (1980) 26; IT-29 (1983) 942.  
Y. Tikochinsky, N.Z. Tishby and R.D. Levine, Phys. Rev. Lett. 52 (1984) 1357.
- [14] C. Fuglesang, Nucl. Instr. Meth. A278 (1989) 765.
- [15] C.S. Lindsey, Nucl. Phys. A544 (1992) 343c.
- [16] NA35 Collab., A. Bamberger et al., Phys. Lett. B205 (1988) 583.
- [17] NA35 Collab., J. Bächler et al., Z. Phys. C51 (1991) 157.
- [18] A. Marzari-Chiesa, Nucl. Phys. A519 (1990) 435c.
- [19] WA80 Collab., R. Albrecht et al., Z. Phys. C55 (1992) 539.
- [20] A. Wróblewski, Acta Phys. Pol. B4 (1973) 857.
- [21] V. Šimák, M. Šumbera and I. Zborovský, Phys. Lett. B206 (1988) 159; in: O. Botner (Ed.), Proceedings of The International Europhysics Conference on High Energy Physics, European Physical Society, Petit-Lancy, Switzerland, 1987.
- [22] P.A. Carruthers, M. Plümer, S. Raha and R.M. Weiner, Phys. Lett. B212 (1988) 369.  
V. Majerník and B. Mamojka, Phys. Scripta 44 (1991) 412.
- [23] M. Pachr, V. Šimák, M. Šumbera and I. Zborovský, Mod. Phys. Lett. A7 (1992) 2333.



- [24] A. Rényi, Probability Theory, North-Holland, Amsterdam, 1970.
- [25] A. Mukhopadhyay, P.L. Jain and G. Singh, Phys. Rev. C47 (1993) 410.
- [26] Z. Daróczy, Inf. Control 16 (1970) 36.  
C. Tsallis, J. Stat. Phys. 52 (1988) 479.  
E.M.F. Curado and C. Tsallis, J. Phys. A24 (1991) L69.

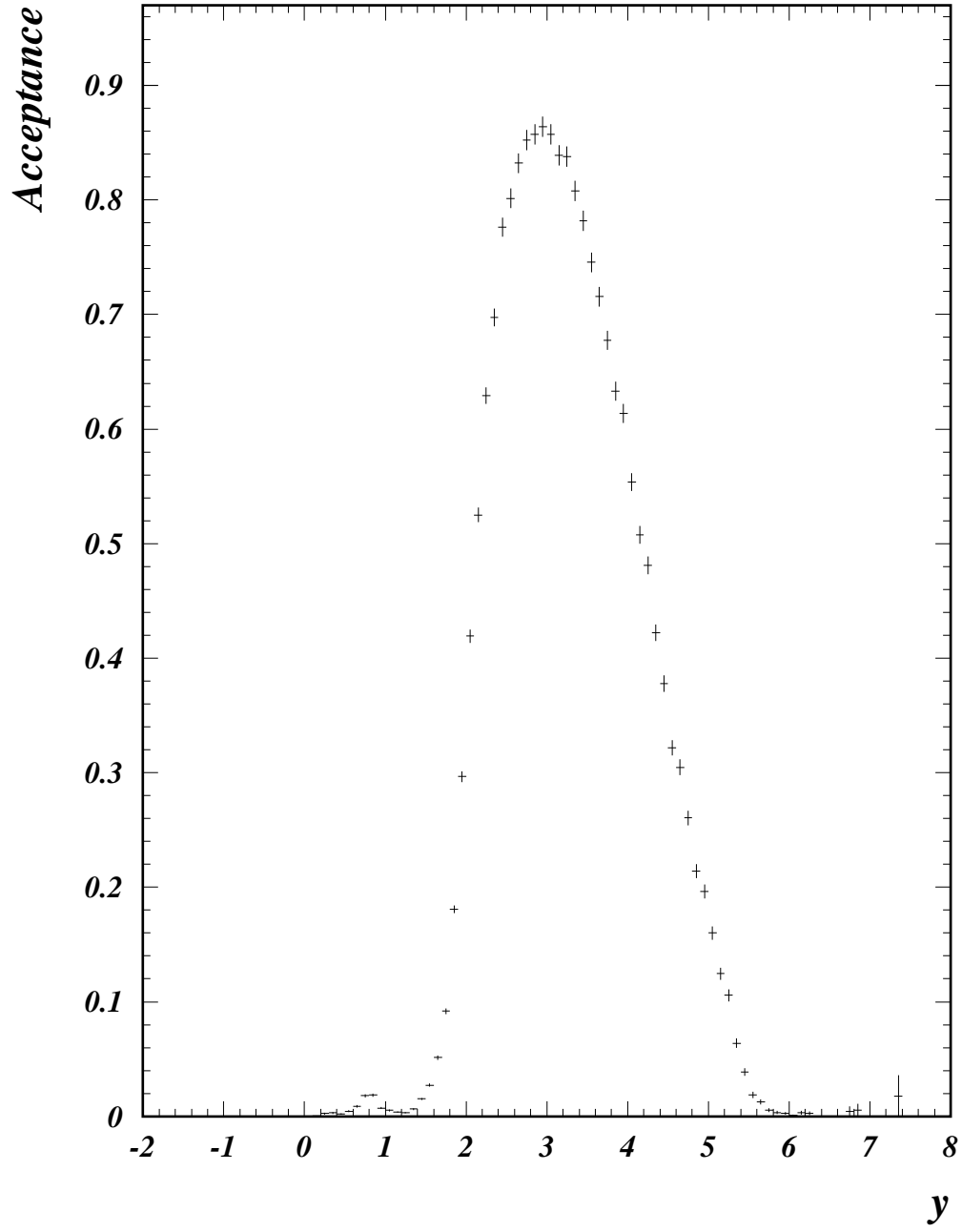


Fig. 1a. The acceptance of the TPC as a function of the laboratory rapidity  $y$

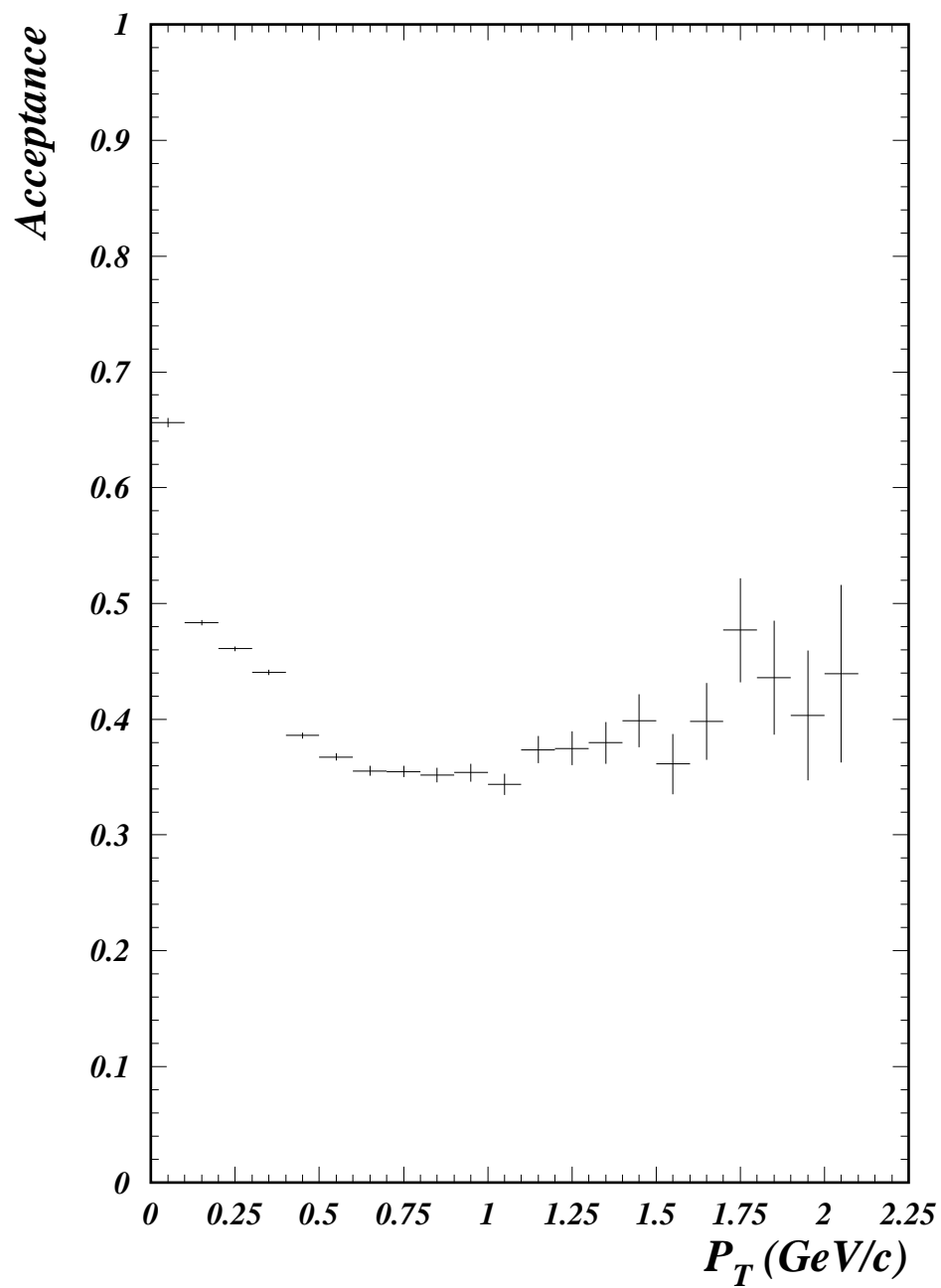


Fig. 1b. The acceptance of the TPC as a function of  $P_T$

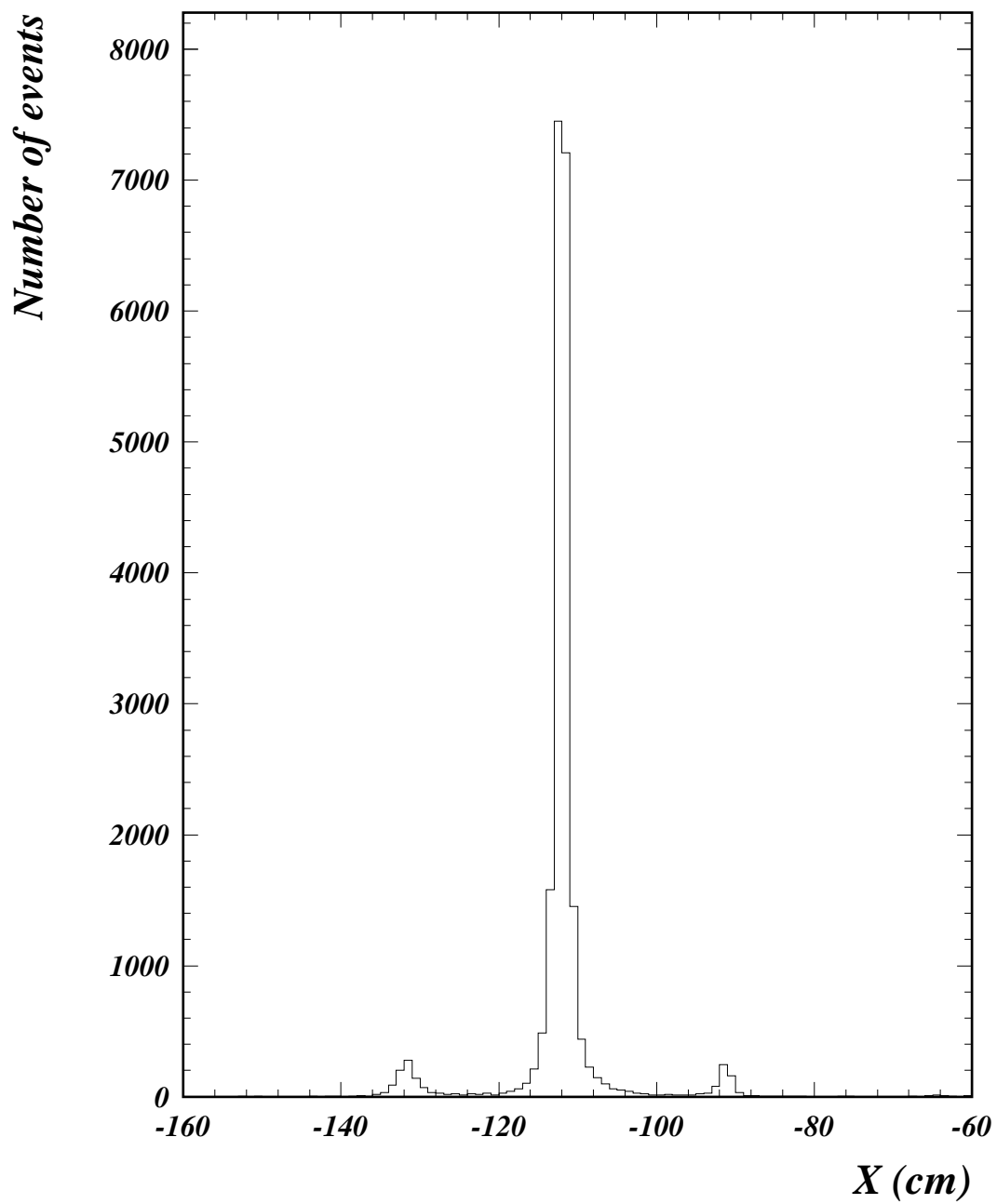


Fig. 2. Distribution of the vertex position  $X$  along the beam direction

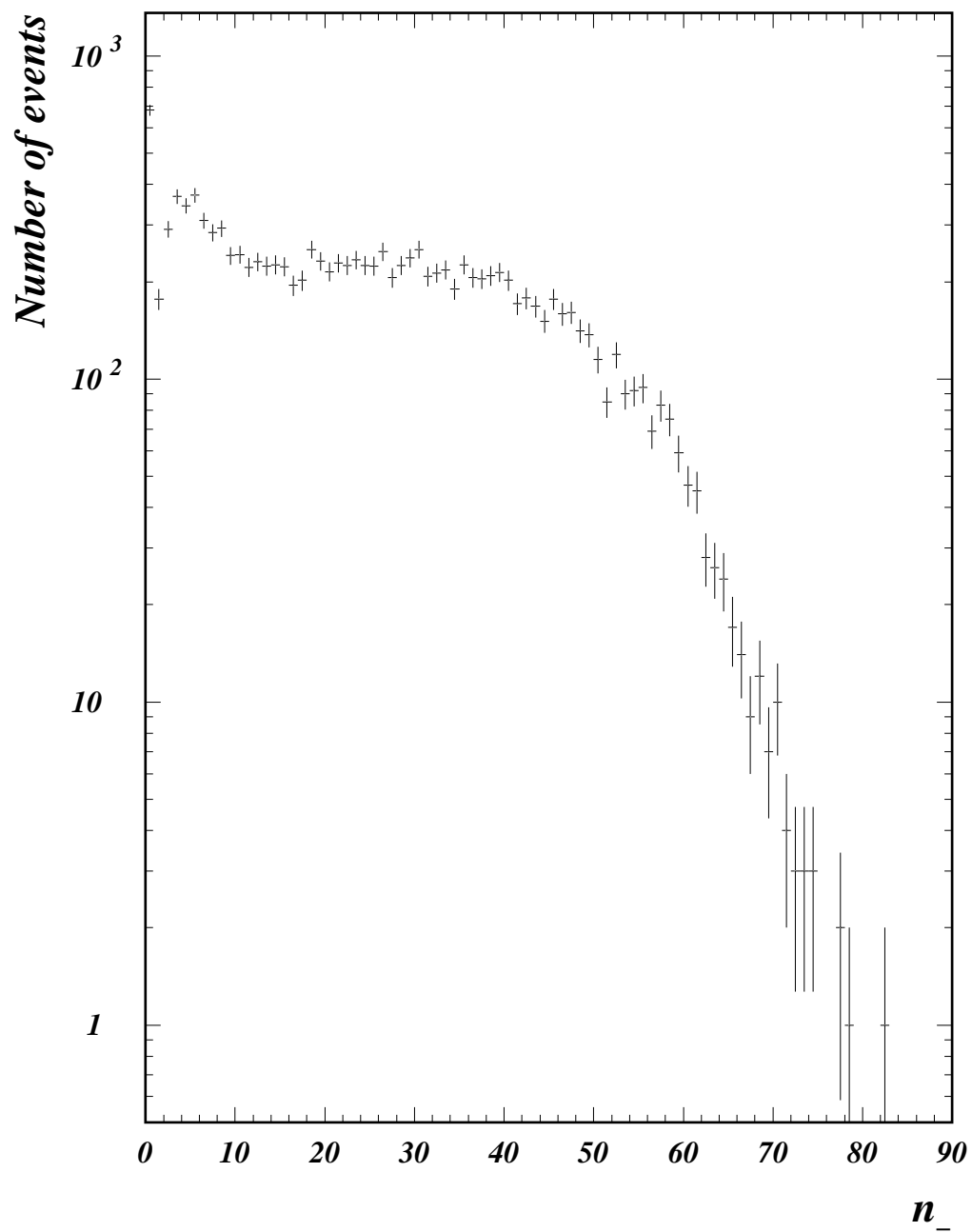


Fig. 3. Observed negative multiplicity distribution

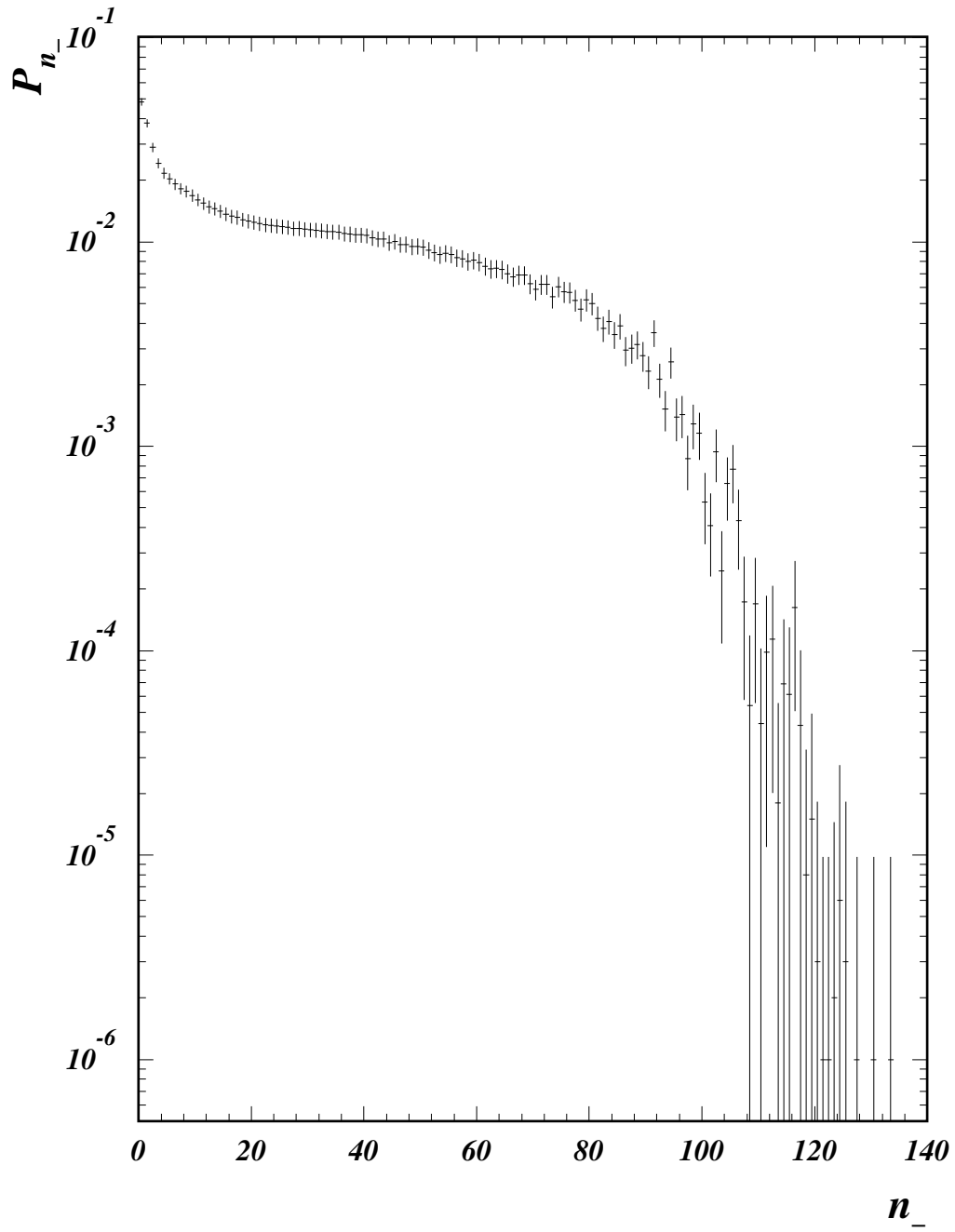


Fig. 4. The corrected negative multiplicity distribution for the TPC phase space

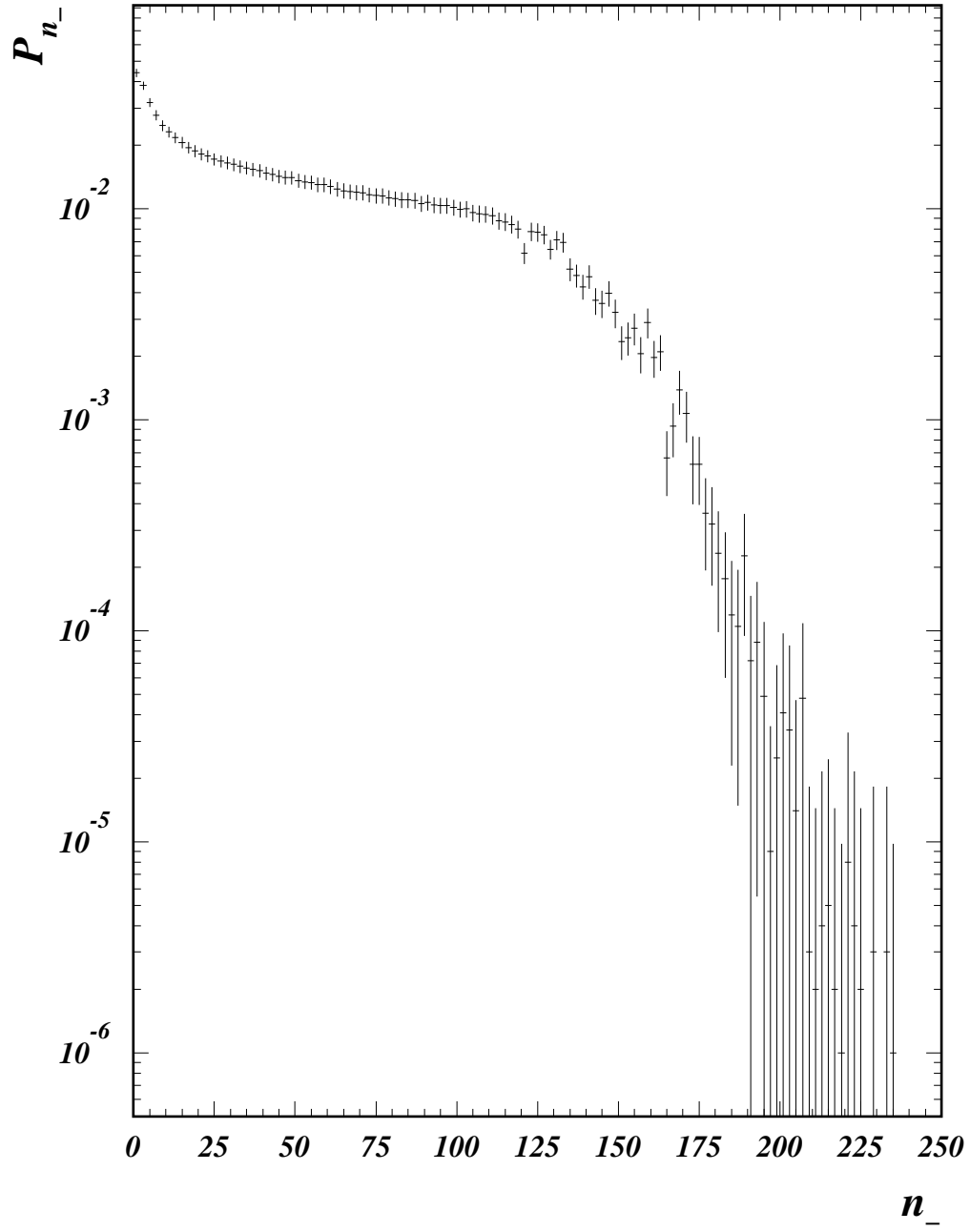


Fig. 5. The corrected negative multiplicity distribution for full phase space

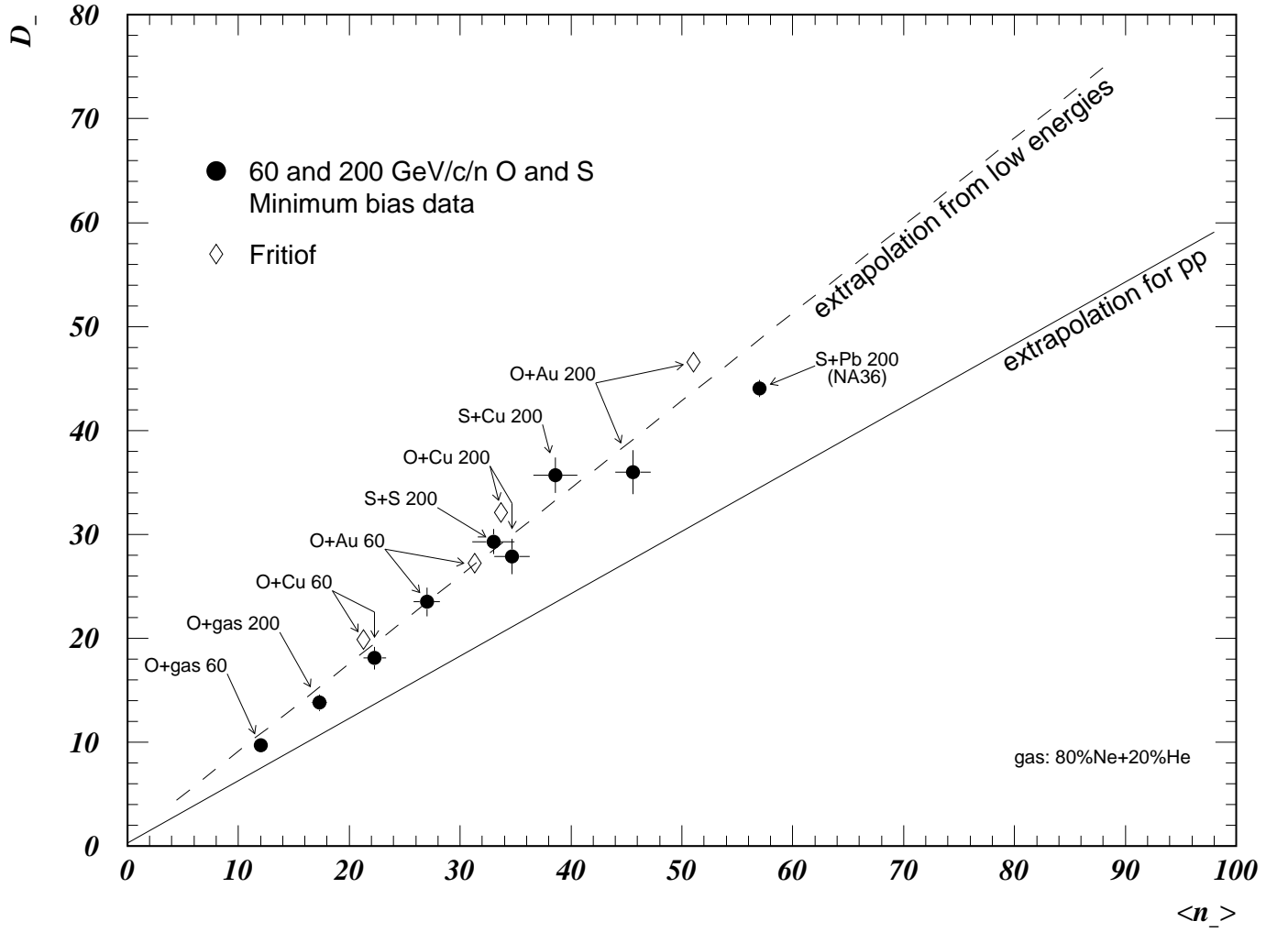


Fig. 6.  $D_-$  as a function of  $\langle n_- \rangle$  for O and S projectiles and different targets, including the result of the present analysis of S-Pb interactions



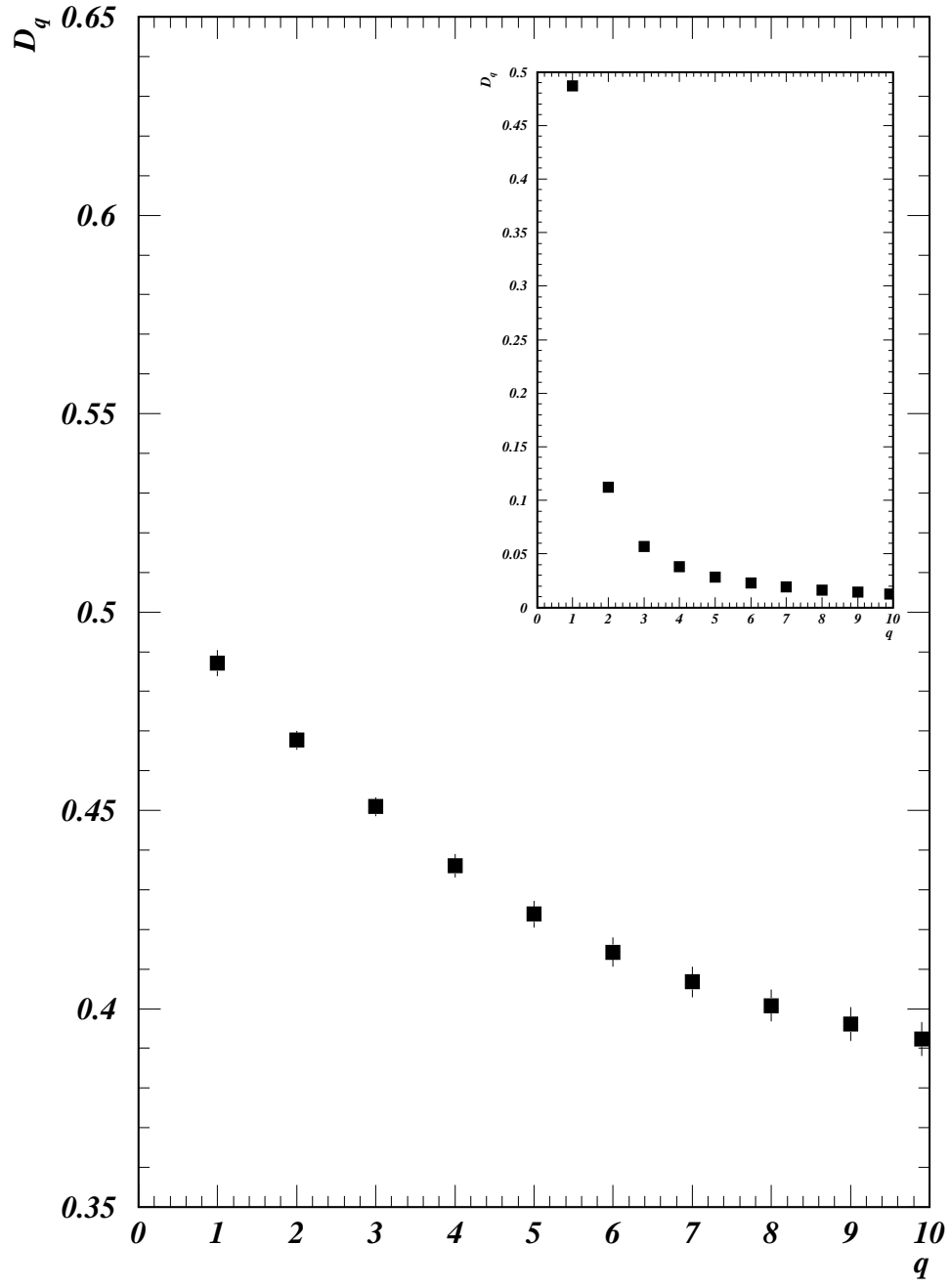


Fig. 7. Generalized fractal dimensions based upon Renyi generalized entropy; the insert gives those from Tsallis generalized entropy